*Journal of Experimental Botany, Vol. 59, No. 14, pp. 4029–4043, 2008*
doi:10.1093/jxb/ern244 Advance Access publication 3 October, 2008
This paper is available online free of all access charges (see http://jxb.oxfordjournals.org/open_access.html for further details)

Journal of Experimental Botany
www.jxb.oxfordjournals.org

**RESEARCH PAPER**

# An autophagy-associated Atg8 protein is involved in the responses of *Arabidopsis* seedlings to hormonal controls and abiotic stresses

**Silvia Slavikova*, Shai Ufaz*, Tamar Avin-Wittenberg, Hanna Levanony and Gad Galili†**

*Department of Plant Sciences, The Weizmann Institute of Science, Rehovot 76100, Israel*

Received 24 June 2008; Revised 27 August 2008; Accepted 8 September 2008

## Abstract

**Eukaryotes contain a ubiquitous family of autophagy-associated Atg8 proteins. In animal cells, these proteins have multiple functions associated with growth, cancer, and degenerative diseases, but their functions in plants are still largely unknown. To search for novel functions of Atg8 in plants, the present report tested the effect of expression of a recombinant AtAtg8 protein, fused at its N-terminus to green fluorescent protein (GFP) and at its C-terminus to the haemagglutinin epitope tag, on the response of *Arabidopsis thaliana* plants to the hormones cytokinin and auxin as well as to salt and osmotic stresses. Expression of this AtAtg8 fusion protein modulates the effect of cytokinin on root architecture. Moreover, expression of this fusion protein also reduces shoot anthocyanin accumulation in response to cytokinin feeding to the roots, implying the participation of AtAtg8 in cytokinin-regulated root–shoot communication. External application of cytokinin leads to the formation of novel GFP–AtAtg8-containing structures in cells located in the vicinity of the root vascular system, which are clearly distinct in size and dynamic movement from the GFP–AtAtg8-containing autophagosome-resembling structures that were observed in root epidermis cells. Expression of the *AtAtg8* fusion construct also renders the plants more sensitive to a mild salt stress and to a lesser extent to a mild osmotic stress. This sensitivity is also associated with various changes in the root architecture, which are morphologically distinct from those observed in response to cytokinin. The results imply multiple functions for AtAtg8 in different root tissues that may also be regulated by different mechanisms.**

Key words: Atg8, autophagy, cytokinin, cytokinin signalling, GFP, root architecture.

## Introduction

Autophagy is a multifunctional degradation machinery in eukaryotic organisms (Huang and Klionsky, 2002; Mizushima *et al*., 2002; Wang and Klionsky, 2003; Thompson and Vierstra, 2005; Patel *et al*., 2006; Bassham, 2007; Scherz-Shouval and Elazar, 2007). One of the central proteins of autophagy is Atg8, which is encoded by a single gene in yeast and by large gene families in higher eukaryotes, including mammals and plants (Stromhaug and Klionsky, 2001; Doelling *et al*., 2002; Mizushima *et al*., 2002). The mammalian Atg8 isoforms have been shown to participate in multiple processes, such as intra-Golgi trafficking (Legesse-Miller *et al*., 1998; Elazar *et al*., 2003; Scherz-Shouval and Elazar, 2007), post-mitotic Golgi reassembly (Muller *et al*., 2002; Scherz-Shouval and Elazar, 2007), interaction with receptors, cytoskeleton elements, and polyubiquitin-binding proteins (Mann and Hammarback, 1994; Wang *et al*., 1999; Wang and Olsen, 2000; Ketelaar *et al*., 2004; Mansuy *et al*., 2004; Chen *et al*., 2006; Pankiv *et al*., 2007), and associations with numerous diseases (Shintani and Klionsky, 2004). In contrast, much less is known about the functions of the Atg8 proteins of plants. Using fusion constructs of green fluorescent protein (GFP) to *Arabidopsis Atg8* (*AtAtg8*), it had been shown that under nutrient starvation stresses, AtAtg8 proteins are processed by the Atg4 protease and assembled into autophagosome-resembling structures that are delivered to the vacuoles, in a similar manner to their mammalian and yeast

* These authors contributed equally to this work
† To whom correspondence should be addressed. E-mail: gad.galili@weizmann.ac.il

counterparts (Yoshimoto *et al*., 2004; Contento *et al*., 2005; Su *et al*., 2006). In addition, under nutrient-limiting conditions, the tobacco (*Nicotiana tabacum*) Atg8 had been suggested to be involved in the transport of protein aggregates containing cytochrome $b_5$ to the vacuole (Toyooka *et al*., 2006). Yet, *Atg8* genes, like other autophagy-associated genes, are also actively expressed in plants under normal growth conditions and their encoded Atg8 proteins are incorporated into autophagosome-resembling structures inside vacuoles (Slavikova *et al*., 2005; Inoue *et al*., 2006), implying a multifunctional role for these proteins in plants, similarly to animals.

To search for novel functions of Atg8 in plants, *Arabidopsis* plants expressing an *Arabidopsis* Atg8f isoform fused at its N-terminus to GFP and at its C-terminus to a haemagglutnin (HA) epitope tag (GFP–AtAtg8f-HA) (Slavikova *et al*., 2005) were subjected to external feeding of cytokinin or auxin as well as to salt and osmotic stresses. The results show that GFP–AtAtg8f-HA expression modulates root architecture as well as shoot anthocyanin accumulation in response to external feeding of cytokinin into the roots. In addition, GFP–AtAtg8f-HA expression appears to render the plants more sensitive to a mild salt stress, and to a lesser extent also to osmotic stress. These results suggest a novel physiological role for autophagy-associated Atg8 proteins in the regulation of root architecture and root–shoot communication.

## Materials and methods

### *Plant material and growth conditions*

Wild-type and transgenic *Arabidopsis* seeds were surface-sterilized in 50% bleach and dispersed on plates containing solid Nitsch medium (Nitsch, 1970) with 2% sucrose and 50 mg $ml^{-1}$ kanamycin. The plates were incubated for 2 d at 4 °C in the dark in order to break seed dormancy. The plates were then transferred to a growth chamber under a long-day regime of a 16 h light/8 h dark cycle at 24 °C, and light intensity of ~30 $\mu Exm^{-2}$ $s^{-1}$. To eliminate potential problems of co-suppression, seeds were first germinated on medium containing kanamycin for ~7–10 d and well-developed seedlings were then transferred either to new plates with the same medium lacking kanamycin or to soil, and subjected to the different experiments described in the Results. The short-day regime included growth under a 12 h light/12 h dark cycle at 24 °C.

For exposure to N starvation conditions, 7-day-old seedlings grown on Nitsch medium containing 2% sucrose and 50 mg $ml^{-1}$ kanamycin in the long-day regime were transferred to N-deficient medium containing: Murashige and Skoog micronutrient salts, 3 mM $CaCl_2$, 1.5 mM $MgSO_4$, 1.25 mM $KH_2PO_4$, 5 mM KCl, 2 mM MES (pH 5.7) for the length of time indicated in the Results. The short-day regime included growth on a 12 h light/12 h dark cycle at 24 °C.

### *Root analysis*

Seedlings were grown vertically in plates and the position of the main root was labelled on the plates every 72 h using a marker in order to follow its growth. The main root length was measured after 10 d, and the number of adventitious and lateral roots was counted under a binocular microscope. Measurements included at least 40 different plants per genotype.

### *Concanamycin A treatment, confocal microscopy, and light microscopy*

Concanamycin A treatment and confocal microscopy were performed as described previously (Slavikova *et al*., 2005).

For light microscopy analysis, roots and their nodule-resembling structures were fixed in 4% paraformaldehyde and 4% dimethylsulphoxide (DMSO) in phosphate-buffered saline (PBS) at pH 7.0. A vacuum was applied to the samples for 15 min and released slowly. After 24 h, samples were rinsed in PBS and dehydrated in an ethanol series of 30, 40, 50, 60, 70, and 85% (60 min each), then incubated overnight in 95% ethanol plus eosin, and finally rinsed four times in 100% ethanol plus eosin for 60 min each. The samples were then processed in a Histoclear series (25, 50, 75, and 100%) for 60 min each and subsequently in Histoclear containing increasing volumes of Paraplast chips (0.25, 0.5, and 0.75 vol.) at 42 °C first and then at 60 °C for several hours each. The samples were then placed in freshly melted wax (paraplast), which was changed twice a day for 3 d at 60 °C. Finally, samples were placed in moulds and stored at 4 °C.

Sections of 8 μm were obtained with a Leica RM 2165 Rotary Microtome. Ribbons of sections were floated on top of double-distilled water and allowed to adhere to Probe On Plus Slides for at least 48 h, at 40 °C. Before staining, the sections were deparaffinized and rehydrated in a Histoclear series (100% and 50%) and in an ethanol series (100, 95, and 70%), and then in double-distilled water. Sections were stained with 1% safranin for 1–3 min, then rinsed thoroughly in double-distilled water. The sections were dehydrated in ethanol (100% and 95%) and then dipped in Histoclear and mounted with Entellan. Sections were examined using a Nikon Eclipse E800 light microscope, and photographs were obtained with an Optronics camera.

### *Conductivity measurement*

Electrolyte leakage in the seedlings was estimated as previously described (Cao *et al*., 2007). Seedlings were agitated in double-distilled water for 30 min on an orbital shaker and the electrolyte loss in liquid was measured with a conductivity meter (C1) (Electronic Switchgear, London). After this conductivity measurement, the samples were boiled at 100 °C for 10 min, then cooled thoroughly at room temperature and the conductivity of the liquid was measured again (C2). The relative electrolyte leakage values were calculated as the C1/C2 ratio.

### *Anthocyanin analysis*

Anthocyanin extraction and estimation was performed as previously described (Laxmi *et al*., 2006). Well-germinated seedlings were transferred to plates containing Nitsch medium with 2% sucrose and 100 ng $ml^{-1}$ zeatin. After 10 d of growth, seedlings were weighed and used for anthocyanin extraction with 3 ml of 1% (v/v) of acidic methanol overnight. The following day, 3 ml of chloroform and 2 ml of double-distilled water were added to the extract. After phase separation, the top aqueous phase was used for spectrophotometrical measurements at 530 nm and 657 nm with a V-630 spectrophotometer (Jasco, USA). The total amount of anthocyanin was calculated as $A_{530}$ minus $A_{657}$ $g^{-1}$ fresh weight.

### *RNA extraction, cDNA synthesis, and quantitative RT-PCR analysis*

Total RNA was extracted from frozen plant tissue using an SV Total RNA Isolation kit (Promega) according to the manufacturer's

instructions. cDNA was synthesized using 3 μg of total RNA as a template with oligo(dT) primer and AMV reverse transcriptase (CHIMERx) according to the manufacturer's instructions. Real-time quantitative PCRs were performed in an optical 96-well plate using the ABI PRISM 7300 Sequence Detection System (Applied Biosystems, Scoresby, Victoria, Australia) and SYBR Green I for monitoring double-stranded DNA synthesis. For all PCRs, the following standard thermal profile was used: 50 °C for 2 min; 95 °C for 15 min; 40 cycles of 95 °C for 15 s and 60 °C for 1 min. In order to compare data from different cDNA samples, $C_T$ (threshold cycle) values for all genes were normalized to the $C_T$ values of cyclophilin (At2g36130), which was used as internal reference in all experiments. Oligonucleotides used for amplification of cyclophilin cDNA were 5′-TGGCGAACGCTGGTCCTAATA-CA-3′ and 5′-CAAAAACTCCTCTGCCCCAATCAA-3′. All primers were designed using the Primer Express 2.0 software (Applied Biosystems). The sequence of sense and antisense primers corresponded to two consecutive exons of the studied genes excluding any genomic DNA amplification. The real-time PCR data were analysed using the comparative $C_T$ method with appropriate validation experiments performed beforehand (Applied Biosystems, User Bulletin #2, http://home.appliedbiosystems.com/). All experiments were repeated at least three times with cDNA templates prepared from three independent batches of plants, and every reaction was set up in duplicate.

Primers used for the qRT-PCR analysis include: phenylalanine ammonia lyase 1 (PAL1; AT2G37040) forward primer (FP), 5′-AAGCCTGAGTTCACCGATCATC, reverse primer (RP), 5′-TAC-GAGCTTCCGTCGAGGAT; chalcone synthase (CHS; AT5G13930) FP, 5-GGAGAAGTTCAAGCGCATGTG, RP, 5-CATGTGACGTT-TCCGAATTGTC; and dihydroflavonol 4-reductase (DFR) (AT5G42800) FP, 5′-TTCCTCTCATGATGCAACCATTC, RP, 5′-GATTCTCATCAACACCTTCAAACGT.

## Results

### *Effect of expression of the GFP–AtAtg8f-HA polypeptide on the response of* Arabidopsis *plants to limiting nitrogen levels and a short-day regime*

Autophagy is known as a multifunctional mechanism that is associated with many other physiological and cellular processes in eukaryotes (Huang and Klionsky, 2002; Mizushima *et al*., 2002; Wang and Klionsky, 2003; Thompson and Vierstra, 2005; Patel *et al*., 2006; Bassham, 2007; Scherz-Shouval and Elazar, 2007). A key regulatory component in autophagy is Atg8, which not only functions in the biogenesis of starvation-induced autophagosomes, but also plays an important role in the cross-talk between autophagy and other cellular and physiological networks through its physical interactions with multiple cellular components. The aim of the present report was to elucidate novel Atg8-mediated cross-reactions of autophagy with various physiological and hormonal processes in *Arabidopsis* plants. Since *Arabidopsis* plants possess nine Atg8 isoforms, which renders suppression approaches unfeasible, the present study used transgenic plants expressing a single AtAtg8f isoform fused at its N-terminus to GFP and at its C-terminus to three copies of the HA epitope tag (GFP–AtAtg8f-HA) under the control of the 35S promoter. These transgenic plants have been described previously (Slavikova *et al*., 2005).

Limiting nitrogen and carbon levels are known to stimulate autophagy, and it has been shown previously that knockout mutants in a number of proteins belonging to the core machinery of autophagy render *Arabidopsis* plants more sensitive to nitrogen and carbon starvation (Doelling *et al*., 2002; Hanaoka *et al*., 2002; Yoshimoto *et al*., 2004; Thompson and Vierstra, 2005; Phillips *et al*., 2008). Hence, the effect of expression of the GFP–AtAtg8f-HA construct on the response of the plants to nitrogen-limiting conditions and to a short-day regime that limits photosynthesis was first tested. As a control, transgenic plants expressing a non-related gene encoding a β-glucoronidase (GUS) reporter protein (hereafter termed 'control' plants) were used. Control and GFP–AtAtg8f-HA seedlings were germinated on Nitsch medium containing kanamycin for 7 d to eliminate potential problems of co-suppression and then well-developed seedlings were transferred to new regular (+N) and N-deficient (–N) Nitsch media for increasing lengths of time. As shown in Fig. 1A, on both the +N and –N media, the GFP–AtAtg8f-HA plants grew to a slightly larger size than the control plants and also growth on –N medium delayed the development of a flowering stem in the control, but not in the GFP–AtAtg8f-HA plants (compare right and left panels in the upper and lower pairs). To test the effect of carbon limitation on the growth of the control and GFP–AtAtg8f-HA plants, well-developed 7-day-old seedlings, germinated on kanamycin-containing medium, were transferred to soil and grown in a growth room under a short-day regime to limit photosynthesis. Also under these growth conditions, the GFP–AtAtg8f-HA-expressing plants had significantly larger shoots and leaves, and also developed the first flowering stem significantly earlier than the control plants (Fig. 1B, C). The size of the leaf epidermis cells, as determined by scanning electron microscopy, was comparable between the two genotypes, indicating that the larger leaf size of the GFP–AtAtg8f-HA plants was mostly due to a larger number of cells (Fig. 1D). Next, seedlings that were germinated on Nitsch medium containing kanamycin for 7 d were transferred to soil, left to grow under short-day conditions for an additional 4 weeks to maintain a relatively low level of fixed carbon, and then transferred to darkness for up to 13 d. Growth under the short-day regime again resulted in larger leaf size in the GFP–AtAtg8f-HA plants compared with the control plants (Fig. 1E; compare top and bottom left panels; 0 days). Yet, transfer to darkness had no marked effect on the senescence of the GFP–AtAtg8f-HA plants, compared with the control plants, and in fact the GFP–AtAtg8f-HA plants tended to be slightly greener than the control plants upon exposure to the dark (Fig. 1E; compare top and bottom panels of 3–13 days). Hence, in

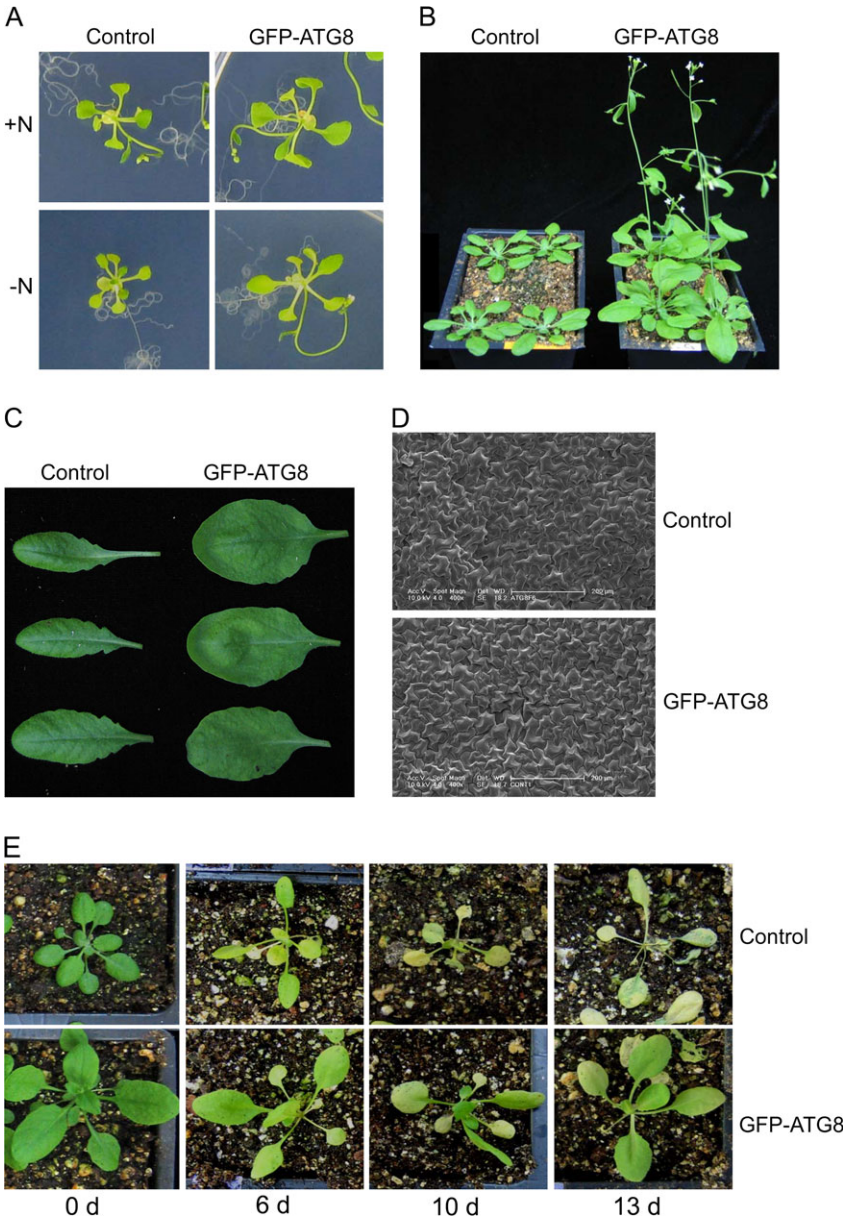


**Fig. 1.** Effect of expression of the GFP–AtAtg8f-HA polypeptide on the response of *Arabidopsis* plants to limiting nitrogen levels and short day regime. (A, B) Morphology of representative control and *GFP–AtATG8-HA*-expressing plants germinated on Nitsch medium containing kanamycin for 7 d and then transferred to N– medium for 2 weeks under a long-day photoperiod (A) or to soil for 4 weeks under a short-day photoperiod (B). (C) The three oldest fully expanded rosette leaves from representative plants described in B. (D) Scanning electron microscopy pictures taken from 6-week-old fully expanded rosette leaves of control and *GFP–AtATG8-HA*-expressing plants grown as described in B. Representative pictures from five different leaves that were each sampled in three different areas are shown. (E) Survival under carbon-limiting growth conditions induced by extended darkness. Control and *GFP–AtATG8-HA*-expressing seedlings, germinated on Nitsch medium containing kanamycin for 7 d, were transferred to soil for an additional 4 weeks under a short-day photoperiod, and then transferred to the dark for the indicated length of time.

contrast to autophagy-deficient *atg* knockout mutants, which are generally slightly smaller, flower later, senesce earlier, and are more sensitive to both N starvation and a short-day photoperiod than wild-type plants (see Thompson and Vierstra, 2005; Downes and Vierstra, 2005, and references therein), expression of GFP–AtAtg8f-HA under the 35S promoter enhances plant growth (leaf size), does not enhance senescence under limiting nutrient stress, and accelerates flowering under nutrient-limiting and short-day growth conditions. This implies that GFP–AtAtg8f-HA expression may enhance autophagy at least with respect to these physiological processes. The only deviation from the above *atg* knockout phenotypes is the *Atatg9* knockout mutant, which possesses an accelerated rather than a delayed flowering (Hanaoka *et al*., 2002).

### *GFP–AtAtg8f-HA expression affects the cytokinin-mediated regulation of root architecture and root–shoot communication*

Previous studies assigned a dominant role to cytokinins in regulating root nitrogen metabolism and nitrogen-mediated long-distance root–shoot communication (Forde, 2002; Moore *et al*., 2003; Franco-Zorrilla *et al*., 2005; Fujita *et al*., 2006; Sakakibara, 2006; Sakakibara *et al*., 2006; Merchan *et al*., 2007; Glover *et al*., 2008). In light of the significant physiological link between autophagy and nitrogen status, it was interesting to test whether GFP–AtAtg8f-HA expression cross-reacts with cytokinin activity. To address this, well-developed control and GFP–AtAtg8f-HA plants were germinated on kanamycin-containing medium for 7 d and then transferred to new medium containing cytokinin (100 ng ml$^{-1}$ zeatin). In the absence of exogenous application of zeatin, the GFP–AtAtg8f-HA-expressing plants and the control plants had relatively comparable root architecture (Fig. 2A, compare left and right sections). Yet, treatment with zeatin caused a significantly stronger retardation of the growth of the primary roots in the GFP–AtAtg8f-HA-expressing plants than in the control plants (Fig. 2B, compare left and right sections). More detailed root quantitative analysis showed the following: (i) in the absence of exogenous application of zeatin, the GFP–AtAtg8f-HA-expressing plants had similar lengths of primary roots, compared with the control plants, a small, but significantly higher number of adventitious roots, and a slightly, but significantly lower, number of lateral roots (Fig. 3A–C; histograms on the

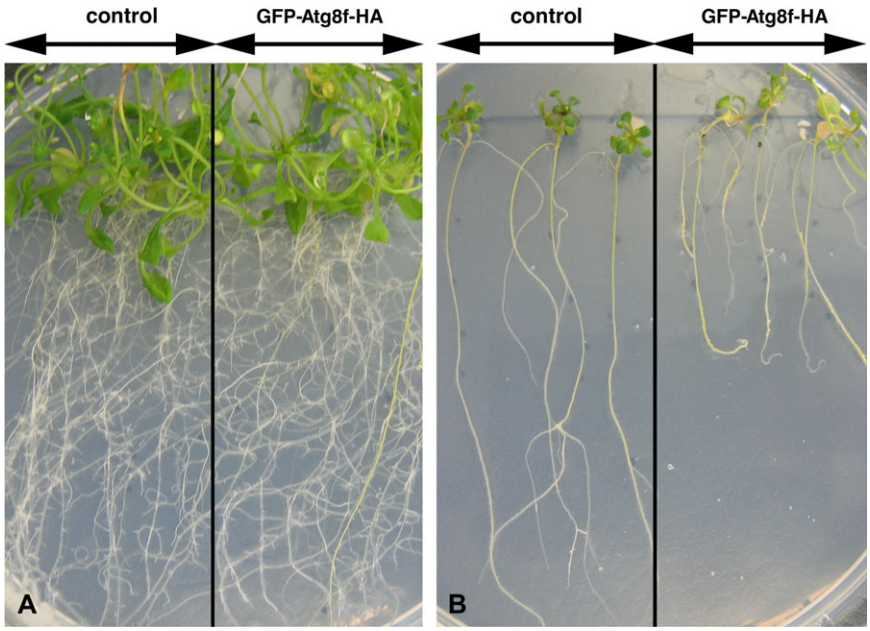


**Fig. 2.** Effect of the cytokinin molecule zeatin (100 ng ml$^{-1}$) on root architecture of the control and GFP–AtAtg8f-HA-expressing plants. A and B show control (left panels) and GFP–AtAtg8f-HA-expressing plants (right panels) grown on medium lacking or containing zeatin, respectively.

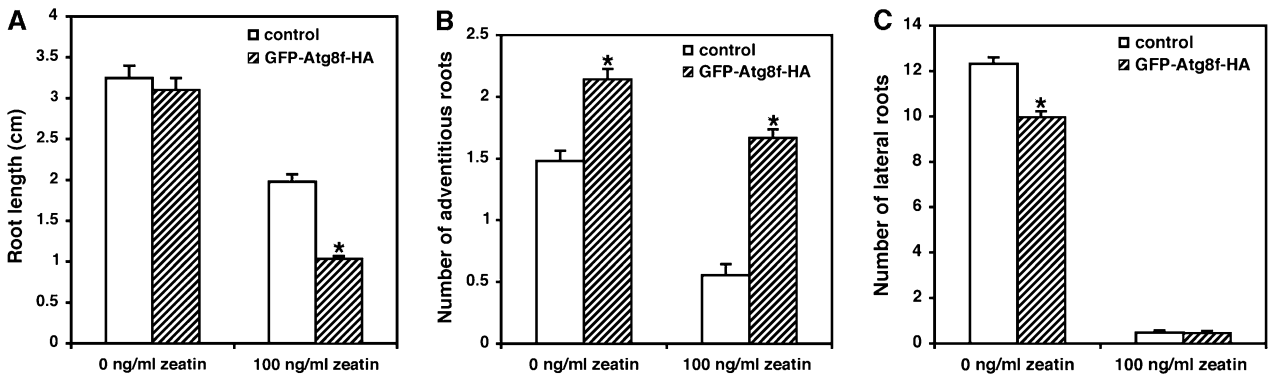


**Fig. 3.** Effect of the cytokinin molecule zeatin (100 ng ml$^{-1}$) on root architecture of the control (white histograms) and GFP–AtAtg8f-HA- (grey histograms) expressing plants. (A) Length of primary roots; (B) number of lateral roots; (C) number of adventitious roots. Bars on the top of the histograms represent the standard error, while asterisks on the top of the histograms represent statistically significant differences ($P$ <0.01).

left); and (ii) exogenous application of zeatin reduced the length of primary roots as well as the number of lateral and adventitious roots in both genotypes, but the extent of inhibition was stronger in the primary roots, similar in the lateral roots, and smaller in the adventitious roots of the GFP–AtAtg8f-HA-expressing plants compared with the control plants (Fig. 3A–C; histograms on the right).

The effect of exogenous application of the auxin molecule indole acetic acid (IAA) on root architecture was also tested. IAA generally had an opposite effect on root architecture to that of zeatin, but this effect was essentially comparable between the GFP–AtAtg8f-HA-expressing plants and the control plants (data not shown).

It was also tested whether GFP–AtAtg8f-HA expression affects cytokinin-mediated root–shoot communication. Feeding of cytokinins to roots is known to stimulate anthocyanin production in shoots, a process that apparently occurs by transmission of the cytokinin signals from the roots to the shoots (Deikman and Hammer, 1995*a*; Laxmi *et al*., 2006). Therefore, the extent of accumulation of shoot anthocyanins in response to application of cytokinin (100 ng $ml^{-1}$ zeatin) to the growth medium was tested in the control and GFP–AtAtg8f-HA plants. Well-developed seedlings, germinated on kanamycin-containing media for 7 d, were transferred to new medium lacking or containing 100 ng $ml^{-1}$ zeatin. As shown in Fig. 4, the effect of zeatin on shoot anthocyanin production was significantly retarded in the GFP–AtAtg8f-HA-expressing plants, compared with the control plants. The reduced accumulation of anthocyanins could also be clearly visualized by the weaker red colour of the shoot anthocyanin extracts (Supplementary Fig. S1 available at *JXB* online).

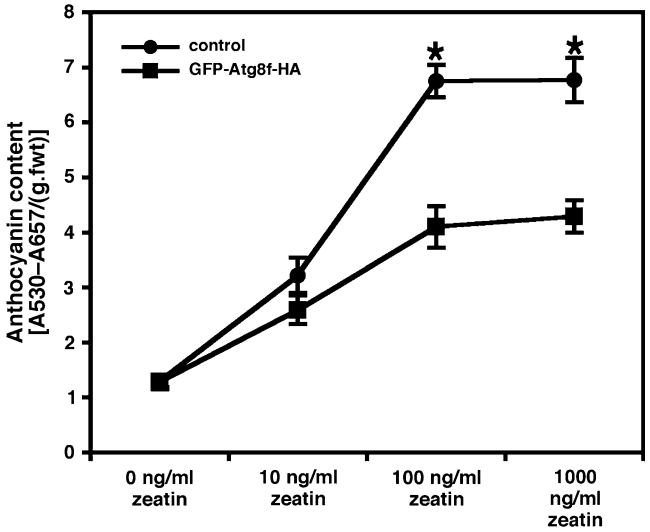


**Fig. 4.** Effect of application of the cytokinin molecule zeatin to the growth medium on anthocyanin content in shoots of the control (circles) and GFP–AtAtg8f-HA-expressing plants (squares). Anthocyanin content was measured spectrophotometrically as $(A_{530}–A_{657})$ $g^{-1}$ fresh weight. Bars represent the standard error and asterisks represent statistically significant differences ($P$ <0.01) between the values of the GFP–AtAtg8f-HA-expressing plants and the control.

Anthocyanins belong to the phenylpropanoid secondary metabolites, which are produced through a chain of enzymatic steps from phenylalanine (Fig. 5A). Among the enzymes of anthocyanin biosynthesis, CHS, DFR, and, to a lesser extent, the more upstream enzyme PAL represent major regulatory steps in shoot anthocyanin accumulation in response to cytokinin application because the genes encoding them are significantly induced by this treatment (Deikman and Hammer, 1995*a*; Holton and Cornish, 1995). To test whether the negative effect of GFP–AtAtg8f-HA expression on shoot anthocyanin accumulation in response to zeatin application to the growth medium is due to altered expression of these genes, qRT-PCR analysis was perormed on RNA extracted from shoots of the control and the GFP–AtAtg8f-HA-expressing plants grown on medium either containing or lacking zeatin (100 ng $ml^{-1}$). As shown in Fig. 5B, the mRNA levels of CHS and DFR, after 10 d exposure to zeatin, were significantly lower by 2.5-fold and 4-fold, respectively, in the GFP–AtAtg8f-HA-expressing plants, compared with the control plants. In addition, a similar reduction trend, even though not significant, was observed in the PAL mRNA level, implying a negative effect of the GFP–AtAtg8f-HA polypeptide on cytokinin-mediated induction of genes encoding early enzymes in the anthocyanin biosynthetic pathway.

Taking into account the influence of GFP–AtAtg8f-HA expression on the effect of zeatin on root architecture and the zeatin-mediated shoot anthocyanin production (Figs 2–5 and Supplementary Fig. S1 at *JXB* online), it was also interesting to test the effect of zeatin on the pattern of accumulation of GFP–AtAtg8f in the roots by confocal microscopy. To address this, well-developed ~5-d-old seedlings of transgenic *Arabidopsis* plants expressing the GFP–AtAtg8f-HA construct, as well as control plants expressing free GFP, were transferred to new medium containing or lacking 100 ng $ml^{-1}$ zeatin for another 10 d. Roots of these seedlings were treated with concanamycin A and analysed by confocal microscopy. This compound enables the visualization of the GFP-fluorescing autophagosome-resembling structures inside vacuoles by inhibiting the activities of vacuolar ATPases and hence slowing down the acidification of the vacuole sap (Drose *et al*., 1993; Yoshimoto *et al*., 2004; Slavikova *et al*., 2005). Root epidermis cells of the GFP–AtAtg8f-HA-expressing plants, grown without zeatin, showed GFP-fluorescing autophagosome-resembling spots inside the vacuoles (Fig. 6A), confirming a previous report (Slavikova *et al*., 2005). Analysis of deeper optic root sections identified in some cases few GFP-fluorescing spots near the vascular system (Fig. 6B, spots marked by arrowheads). The localization of these spots near the

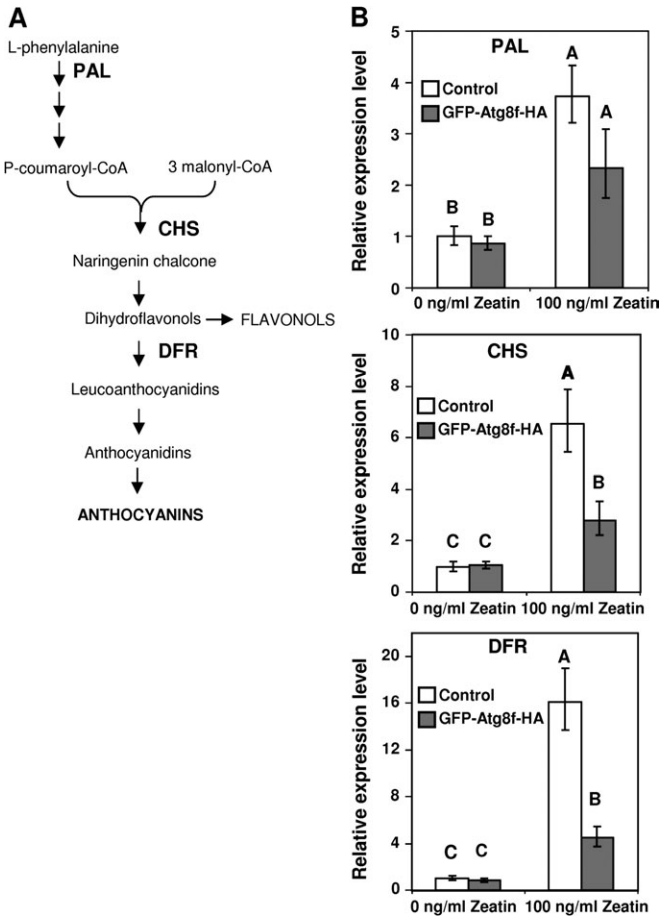


**Fig. 5.** Effect of application of the cytokinin molecule zeatin (100 ng $ml^{-1}$) to the growth medium on the expression of genes encoding three main enzymes of the anthocyanin biosynthetic pathway in shoots of the control and GFP–AtAtg8f-HA-expressing plants. (A) Schematic representation of the flavonoid biosynthetic pathway. The enzymes whose mRNA levels were quantified in B are indicated in bold. (B) RNA was extracted from shoots germinated as described in Fig. 1 and then on medium containing or lacking 100 ng $ml^{-1}$ zeatin for an additional 10 d. Relative mRNA levels of phenylalanine ammonia lyase (PAL1; AT2G37040), chalcone synthase (CHS; AT5G13930), and dihydroflavonol 4-reductase (DFR; AT5G42800) were quantified using qRT-PCR as described in Materials and methods. Values of the mRNA transcript level are relative to that of the control plants grown without zeatin (left open bar). Bars on the top of the histograms represent the standard error, while different letters on top of the histograms represent statistically significant differences ($P$ <0.05).

vascular system was also clearly seen by merging the GFP fluorescence images with differential interference contrast (DIC) images of the same region (Fig. 6C; a xylem vessel is delimited by two opposite facing arrows). The spots near the vascular system were clearly distinct from the autophagosome-resembling structures in the epidermis cells by exhibiting significantly less dynamic movement (data not shown). Treatment with zeatin significantly reduced the amount of GFP-fluorescing autophagosome-resembling structures in the vacuoles of root epidermis cells (Fig. 6D, compare with A). Notably, the zeatin treatment also resulted in the formation of specific GFP–AtAtg8f-containing structures near the vascular system, which were larger than those observed without zeatin treatment (Fig. 6E, F, compare with B, C), but exhibiting a similar low dynamic movement (data not shown). Control seedlings expressing free GFP treated with zeatin (Fig. 6G–I) showed neither GFP-fluorescing autophagosome-resembling structures inside the vacuoles of the root epidermis cells (Fig. 6G) nor GFP-fluorescing bodies in the vicinity of the root vascular system (Fig. 6H, I).

### *Effect of GFP–AtAtg8f-HA expression on the response of plants to salt and osmotic stresses*

Root architecture as well as plant metabolism are also influenced by abiotic stresses (Katsuhara and Kawasaki, 1996; Huh *et al*., 2002; Sanchez *et al*., 2008; Shulaev *et al*., 2008). Hence, the effect of GFP–AtAtg8f-HA expression on the response of plants to salt and osmotic stresses was also tested. Based on calibration analysis (data not shown), a decision was made to use 100 mM and 150 mM NaCl as well as 50 mM and 150 mM mannitol as representatives of relatively mild and more severe salt and osmotic stresses, respectively. Well-developed ~10-day-old seedlings, germinated on kanamycin-containing medium, were transferred to new medium containing 100 mM NaCl (salt stress) or 50 mM mannitol (osmotic stress). As shown in Fig. 7A, panels d and h, in the absence of salt stress, seedlings of the control and the GFP–AtAtg8f-HA-expressing plants grew with relatively comparable phenotypes. Exposure to 100 mM NaCl for up to 30 d had a relatively mild negative effect on the size of the control plants and also caused the characteristic darker green colour resulting from the salt stress (Fig. 7A, compare panels a–c with d). In contrast, exposure to 100 mM NaCl for up to 30 d had a considerably stronger negative effect on growth of the GFP–AtAtg8f-HA-expressing plants, which showed a considerably fainter green colour of their leaves compared with the control plants (Fig. 7A, compare panels a–c with e–g, respectively). The retarded growth phenotype of the GFP–AtAtg8f-HA-expressing plants on medium containing 100 mM NaCl was also associated with increased electrolyte leakage (Fig. 7B), indicating greater damage of the cell membrane system in comparison with the control seedlings (Cao *et al*., 2007).

Upon exposure to the more severe salt stress of 150 mM NaCl, the growth of both the control and the GFP–AtAtg8f-HA plants was severely retarded in a comparable manner, resulting in extensive bleaching of all of the genotypes after 14 d (Supplementary Fig. S2A at *JXB* online; compare panels a–d with the respective panels e–h). Hence, expression of GFP–AtAtg8f-HA renders *Arabidopsis* seedlings more sensitive to the relatively mild, but not the more severe salt stress.

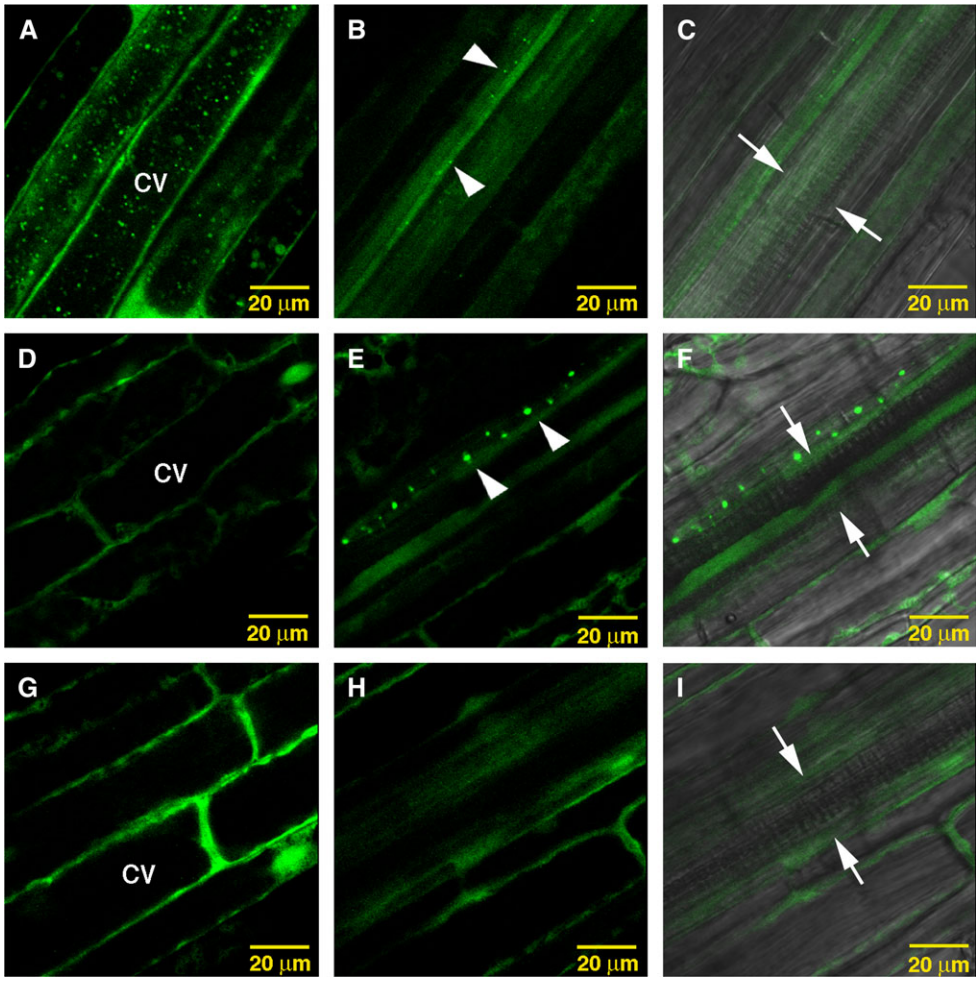


**Fig. 6.** Effect of the cytokinin molecule zeatin on GFP fluorescence in roots of 10-day-old *Arabidopsis* plants expressing either GFP–AtAtg8f-HA (A–F) or free GFP as a control (G–I). Roots were left untreated (A–C) or were treated (D–I) with 100 ng $ml^{-1}$ zeatin. Roots were analysed by confocal microscopy and differential interference contrast (DIC) microscopy following treatment with concanamycin A. (A), (D), and (G) show confocal microscopy optical sections of the root epidermis cells. (B), (E), and (H) show confocal microscopy optical sections in the vicinity of the root vascular system. (C), (F), and (I) represent merging of the confocal microscopy images in the vicinity of the root vascular system (B, E, H) with the identical regions obtained by DIC microscopy. Arrows facing each other in C, F, and I delimit the xylem vessel from both sides. Arrowheads in B and E indicate distinct GFP-fluorescing structures formed in the vicinity of the root vascular system of the GFP–AtAtg8f-HA-expressing plants, but not the control plants, and particularly intensified upon treatment with zeatin. Central vacuoles are indicated as CV.

The effect of expression of the GFP–AtAtg8f-HA construct on the response of the plants to relatively mild (50 mM mannitol) and more severe (150 mM mannitol) osmotic stresses was also tested. The mild osmotic stress slightly retarded the growth of the control and the GFP–AtAtg8f-HA-expressing plants (Fig. 7C, compare panels a–c with d, and panels e–g with h). In addition, it also had a relatively mild negative effect on the growth of the GFP–AtAtg8f-HA-expressing plants, compared with the control plants, which was manifested by enhanced senescence of the older leaves, particularly observed after 30 d exposure to this stress (Fig. 7C, compare panels c and g). Similarly to the more severe salt stress of 150 mM NaCl, the more severe osmotic stress of 150 mM mannitol retarded the growth of both the control and the GFP–AtAtg8f-HA-expressing plants in a comparable manner (Supplementary Fig. S2B at *JXB* online; compare panels a–d with the respective panels e–h).

### *Effects of salt and osmotic stresses on root architecture of the GFP–AtAtg8f-HA-expressing plants*

Exposure of plants to salt stress stimulates changes in root architecture, including shortening of the primary roots and proliferation of secondary roots, an adaptive mechanism that apparently improves the tolerance of the plants to this stress (Huh *et al.*, 2002). It was therefore interesting to test whether the growth retardation of the GFP–AtAtg8f-HA-expressing plants after exposure to 100 mM NaCl was associated with altered response of their roots to the

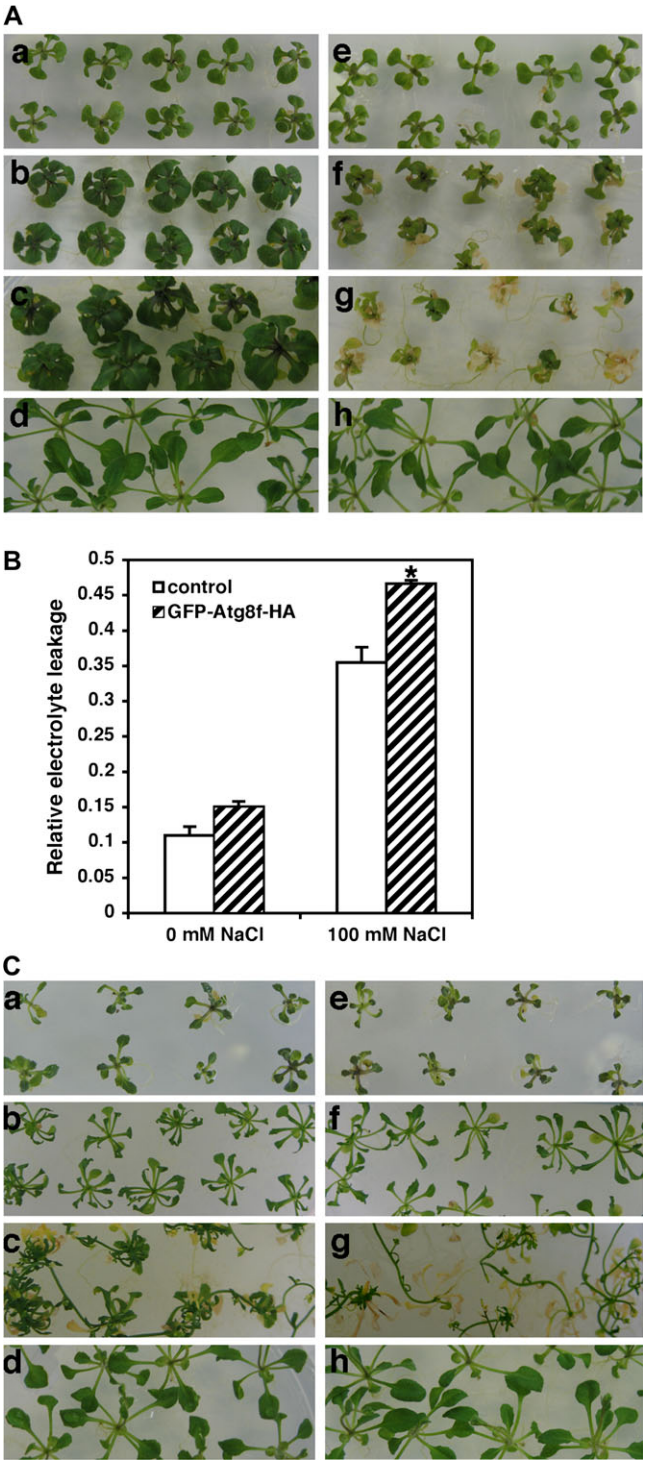


**Fig. 7.** Effect of mild salt and osmotic stresses on the growth of seedlings of control plants and GFP–AtAtg8f-HA-expressing plants. Plants were germinated and transferred to new medium as described in Fig. 1. (A) Morphology of the control plants (a–c) and GFP–AtAtg8f-HA-expressing plants (e–g) upon exposure to a salt stress of 100 mM NaCl for 6 (a, e), 14 (b, f), and 30 (c, g) days. Control plants and GFP–AtAtg8f-HA-expressing plants grown for 14 d without salt stress are shown in panels d and h, respectively. (B) Relative electrolyte leakage analysis of control plants (white histograms) and GFP–AtAtg8f-HA-expressing plants (grey histograms) grown with either no salt (left section) or 100 mM NaCl (right section). Bars on the top of the histograms represent the standard error, while an asterisk on the top of the right histogram represents statistically significant differences ($P$ <0.01). (C) Morphology of the control plants (a–c) and GFP–AtAtg8f-HA-expressing plants (e–g) upon exposure to an osmotic stress of 50 mM mannitol for 6 (a, e), 14 (b, f), and 30 (c, g) days. Control plants and GFP–AtAtg8f-HA-expressing plants grown for 14 d without osmotic stress are shown in panels d and h, respectively.

salt stress. These experiments were performed on plants grown vertically on agar plates. As shown in Fig. 8, upon growth on medium lacking NaCl for 14 d, the root architecture was highly comparable between the control and GFP–AtAtg8f-HA-expressing plants (Fig. 8A, compare left and right sections). Exposure to 100 mM NaCl for 14 d had a considerably stronger retardation effect on the elongation of the primary roots of the control plants, compared with the GFP–AtAtg8f-HA-expressing plants (Fig. 8B, compare the left and right sections).

Exposure to the osmotic stress of 150 mM mannitol for 14 d had no major effect on root growth of either the control or GFP–AtAtg8f-HA-expressing plants (Fig. 8C, compare the left and right sections). However, after prolonged exposure of the GFP–AtAtg8f-HA-expressing plants to 150 mM mannitol for >30 d under the vertical growth condition, the ageing roots of the GFP–AtAtg8f-HA-expressing plants became wider in diameter than the roots of the control plants and also developed specific globular structures that were not observed in roots of the control plants (compare Fig. 8D and E). In rare cases, similar globular structures were also developed upon exposure of vertically grown GFP–AtAtg8f-HA-expressing plants to salt stress (100 mM NaCl) but, under this stress, the structures appeared only after growing on 100 mM NaCl for ~20 d followed by a recovery period in which the plants were transferred back into medium lacking NaCl for an additional ~20 d (data not shown). The reason for these differences is still unknown. These globular structures (Fig. 8E) resemble in their morphology the nodules formed in legumes roots in response to symbiotic interactions with *Rhizobium* bacteria. Moreover, their formation only on roots of the GFP–AtAtg8f-HA-expressing plants, but not on roots of the control plants, is particularly interesting for the following two reasons: (i) *Arabidopsis* plants generally do not form root nodules as do legume plants; and (ii) a gain-of-function mutation in a cytokinin receptor was recently shown to trigger spontaneous root nodule organogenesis in the legume species *Lotus japonicus* in the absence of rhizobial signal molecules (Tirichine *et al*., 2007).

Since cytokinins are known to be associated with cell division, cell proliferation, and organ regeneration (Sakakibara, 2006), it was interesting to test the anatomy of the wider roots and the globular, nodule-like structures of the GFP–AtAtg8f-HA-expressing plants. As shown in Fig. 9A and B, cross-sections showed that after prolonged exposure to osmotic stress, the roots of the GFP–AtAtg8f-HA-expressing

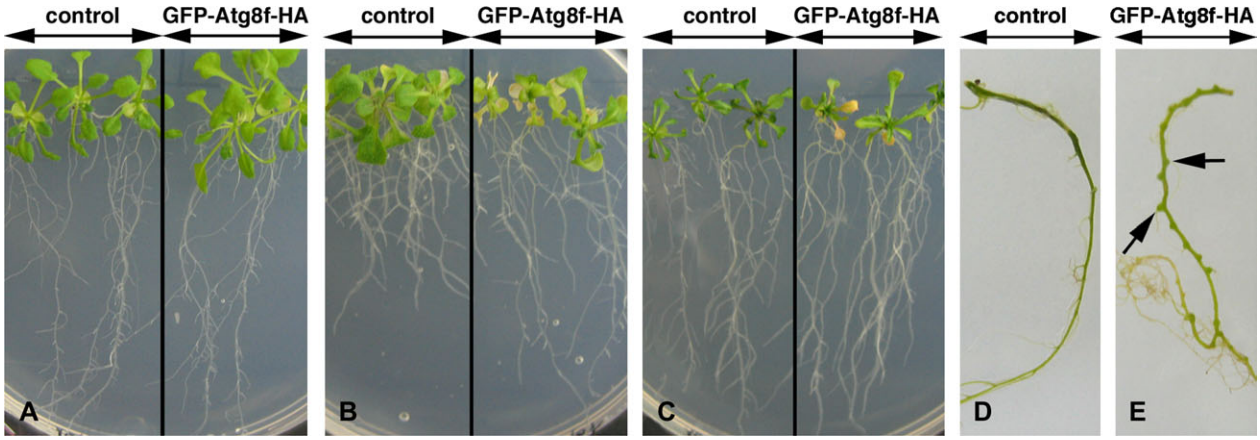


**Fig. 8.** Effect of salt and osmotic stresses on the root architecture of the control and the GFP–AtAtg8f-HA-expressing plants. Plants were germinated as described in Fig. 1 and then transferred and grown vertically for 14 d on medium lacking salt or mannitol (A), containing 100 mM NaCl (B), or containing 150 mM mannitol (C). The left and right sections in each of A–C contain control and GFP–AtAtg8f-HA-expressing plants, respectively. D and E show, respectively, sections of the main roots of the control and GFP–AtAtg8f-HA-expressing plants grown for an extended period of 30 d on medium containing 150 mM mannitol. Arrows in E show the nodule-resembling structures.

plants were nearly 4-fold wider than those of the control plants (see size bars). This was largely due to cell proliferation in the vicinity of the vascular xylem and phloem tissues (compare Fig. 9A and B). Higher magnifications of cross-sections of roots of the GFP–AtAtg8f-HA-expressing plants showed extensive proliferation of viable cells with globular plastids in the vicinity of the xylem and phloem (Fig. 9C–E). Proliferation of cells in the vicinity of the phloem was also visible in a longitudinal root cross-section (Fig. 9F). A longitudinal section in the nodule-resembling structures formed on roots of the GFP–AtAtg8f-HA-expressing plants was then also performed. Sections of the entire structure showed extensive vascular tissues surrounded by large numbers of cells (Fig. 9G), which were then observed more clearly at higher magnifications (Fig. 9H, I).

## Discussion

### *Utilization of plants constitutively expressing GFP–AtAtg8f-HA to elucidate interactions of autophagy with physiological and hormonal processes*

Results from mammalian cells imply that Atg8 proteins possess at least two distinct functions in the autophagic process: (i) they specifically interact with various intracellular proteins to regulate their functions directly. For example, it has been shown that interaction of the mammalian Atg8 isoform GABARAP with GABA (γ-aminobutyric acid) receptors regulates their trafficking and possibly also their clustering on the plasma membrane (Kanematsu *et al*., 2007, and references therein) and that the interaction of another mammalian Atg8 isoform, GATE-16, with a Golgi-associated v-SNARE promotes Golgi reassembly (Muller *et al*., 2002). (ii) Through interacting with their target proteins, the Atg8 proteins also facilitate their internalization into autophagosomes en route towards their degradation inside the vacuole, a process that apparently occurs both during regular growth and in response to nutrient starvation (Mizushima *et al*., 2002). Knockout mutants in various autophagy-associated genes of plants generally render the plants more sensitive to nitrogen and sugar starvation (Thompson and Vierstra, 2005; Downes and Vierstra, 2005; Bassham *et al*., 2006). Hence, the observation that the expression of GFP–AtAtg8f-HA under the 35S promoter improves the growth of plants under nitrogen- and light-limiting conditions implies that this expression apparently enhances classical autophagy under nutrient starvation. This observation also illustrates the specific function of the GFP–Atg8-HA fusion protein in autophagy-associated processes.

Another major aim of this study was to identify novel cellular processes that cross-react with the constitutive autophagy machinery (Slavikova *et al*., 2005; Inoue *et al*., 2006) and that are not directly associated with acute nutrient starvation. To eliminate possible variability in germination vigour between different batches of seeds and also possible co-suppression of the transgene, it was decided to germinate the seeds on kanamycin-containing medium and then transfer only the well-developed seedlings into other media or soil lacking kanamycin. Additional experiments in which the seeds were germinated directly on the experimental medium without kanamycin yielded similar results, but seedling establishment was variable and the observed phenomena were generally milder (data not shown). Hence, it is also concluded that either germination in the presence of kanamycin or the transfer of the seedlings to new plates implemented some stress responses that stimulated the extent of the observed phenomena.

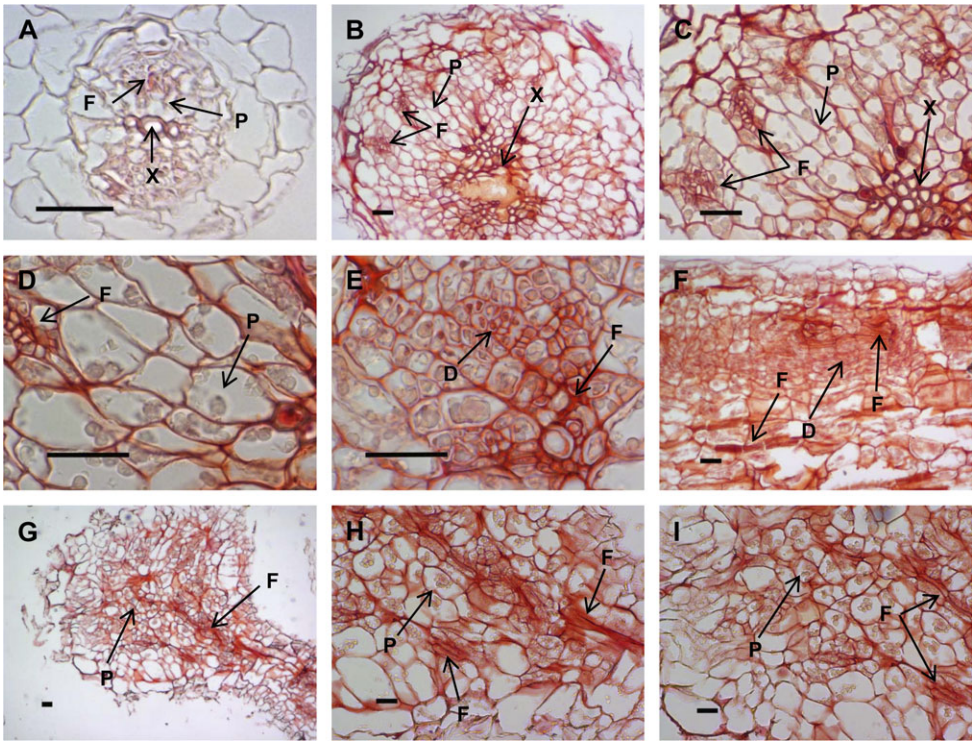


**Fig. 9.** Light microscopy analysis of ageing roots of the GFP–AtAtg8f-HA-expressing plants following exposure to osmotic stress. (A) Cross-section of an ageing root of control plants; (B–E) cross-sections of ageing roots of the GFP–AtAtg8f-HA-expressing plants at different magnifications; (F) a longitudal section of an ageing root of the GFP–AtAtg8f-HA-expressing plants; (G–I) cross-sections of the nodule like structures developed on the ageing roots of the GFP–AtAtg8f-HA-expressing plants. Bars represent 100 μm. D, dividing phloem cells; F, phloem cells; P, parenchyma cells; X, xylem cells.

### *GFP–AtAtg8f-HA expression influences cytokinin-associated processes*

Autophagy is strongly induced during plant senescence, a process that is generally inhibited by cytokinins (Gan and Amasino, 1995). Hence, the observation that zeatin inhibits the incorporation of the GFP–AtAtg8f-HA polypeptide into autophagosome-resembling structures inside the vacuoles of root epidermis cells supports the primary role of autophagy in bulk macromolecule degradation processes occurring during senescence. Yet, cytokinins are associated with multiple additional processes in plants that may be regulated by interactions of specific proteins with the autophagy-associated Atg8 proteins in an analogous manner to the functions of Atg8 proteins in animal cells. Indeed, several independent lines of evidence in this report suggest that expression of the GFP–AtAtg8f-HA construct alters various cytokinin-associated processes in the roots. Zeatin suppressed the growth of primary roots, lateral roots, and adventitious roots in both the control and GFP–AtAtg8f-HA-expressing plants, but the effect of zeatin in the GFP–AtAtg8f-HA-expressing plants was significantly stronger than in the control plants in the primary roots, similar to that in the control plants in the lateral roots and significantly weaker than that in the control plants in the adventitious roots (Fig. 3). These results imply that GFP–AtAtg8f-HA expression may trigger a gradient of cytokinin signalling perception ranging from a stronger perception in the bottom primary roots to a weaker perception in the upper adventitious roots. Alternatively, the increased autophagy due to overexpression of GFP–AtAtg8f-HA may have different effects in different cell types. The nature of this interesting phenomenon awaits future studies.

In addition to controlling root growth, cytokinins also participate in the regulation of long-distance root–shoot communication in response to various metabolic stresses (Moore *et al*., 2003; Franco-Zorrilla *et al*., 2005; Fujita *et al*., 2006; Sakakibara, 2006). Such communication is also exemplified by the observation that feeding of cytokinins to the roots stimulates anthocyanin production in the shoots (Deikman and Hammer, 1995*b*). The results showing that GFP–AtAtg8f-HA expression slows down the synthesis and accumulation of anthocyanins in shoots in response to exogenous zeatin application to the growth medium (Figs 4, 5; Supplementary Fig. S1 at *JXB* online) also support a regulatory role for AtAtg8f in cytokinin-mediated root–shoot communication signals. Such a regulatory role is also supported by a confocal microscopy analysis showing that zeatin treatment triggers the formation of special GFP-fluorescing structures in the vicinity

of the root vascular system in plants expressing the GFP–AtAtg8f-HA construct, but not in control plants expressing free GFP (Fig. 6). In addition, a recent study analysing gene expression in specific *Arabidopsis* root tissues demonstrated a significant expression of several genes involved in cytokinin transport and signalling in root vascular tissues (Brady *et al*., 2007). Taken together, these data raise the possibility that the GFP-fluorescing structures induced by zeatin treatment might sequester proteins involved in cytokinin transport or signalling, thus abrogating root–shoot communication.

The association of the autophagy-associated Atg8 proteins with cytokinin activity is also particularly interesting taking into account the strong physiological association between autophagy and nitrogen metabolism on one hand and the interaction between nitrogen metabolism and cytokinin on the other hand (Sakakibara *et al*., 2006; Hirose *et al*., 2008). A close correlation between nitrogen status and cytokinin content has been reported in a number of plant species (Singh *et al*., 1992; Samuelson and Larsson, 1993; Wagner and Beck, 1993; Takei *et al*., 2001, 2004). In addition, expression of the *Arabidopsis* cytokinin biosynthesis genes IPT3 and IPT5 is regulated by different nitrogen sources (Miyawaki *et al*., 2004; Takei *et al*., 2004).

### *The effects of GFP–AtAtg8f-HA expression on root architecture in response to cytokinin application and salt stress are possibly mediated by distinct mechanisms*

The present results showed that GFP–AtAtg8f-HA expression alters the adjustment of root architecture to both salt stress and exogenous cytokinin application. Yet, while both cytokinins and salt stress generally inhibit the growth of primary roots in wild-type plants (Huh *et al*., 2002; Aloni *et al*., 2006), expression of the GFP–AtAtg8f-HA construct prevented the inhibition of primary root growth under salt stress (Fig. 8B), while accelerating the inhibition of primary root growth in response to zeatin application (Figs 2, 3). Notably, cytokinin treatment also induced the formation of specific bodies containing GFP–AtAtg8f in the vicinity of the root vascular system (Fig. 6). The nature of these bodies is still unknown, but they are clearly distinct from the autophagosome-resembling structures inside the vacuoles of root epidermis cells due to their larger size (Fig. 6) and significantly lower dynamic movement (data not shown). The conceivable differential functionality of these two structures is also supported by the fact that zeatin reduces the accumulation of autophagosome-resembling structures in root epidermis cells while stimulating the production of the larger bodies in the vicinity of the root vascular system (Fig. 6). The protein content and function of the cytokinin-induced GFP–AtAtg8f-containing structures near the root vascular system is still unknown, but similar structures were also found to be associated with various mammalian cancers, diseases, and neurodegenerative disorders (Ohshiro *et al*., 2007; Pankiv *et al*., 2007; Xie and Klionsky, 2007). Exposure of plants to oxidative stress also stimulates autophagy, which is apparently used for selective degradation of damaged proteins (Xiong *et al*., 2007), and it is possible that the cytokinin-induced GFP–AtAtg8f-containing structures near the vascular system contain specific proteins that are targeted for degradation by autophagy. Alternatively, it is possible that Atg8 regulates cytokinin signalling by regulating the intracellular trafficking of specific proteins via the Golgi in a similar manner to the functions of mammalian Atg8 proteins (Legesse-Miller *et al*., 1998; Elazar *et al*., 2003; Scherz-Shouval and Elazar, 2007). Similar structures to the GFP–AtAtg8f-containing bodies were also observed to contain the auxin transporters PIN1 and AUX1 in response to treatment with brefeldin A (BFA; Geldner *et al*., 2001; Grebe *et al*., 2002). This metabolite blocks trafficking from recycling endosomes to the plasma membrane, causing the accumulation of endosomes and internalized endocytic cargo in the so-called BFA compartments (Geldner *et al*., 2001, 2003). However, it is still unknown whether these bodies also contain Atg8.

The mechanism behind the effect of GFP–AtAtg8f-HA on preventing the growth arrest of primary roots in response to salt stress is also still unknown. The inhibition of primary root growth under salt stress enables the proliferation of secondary roots that can better handle the salty environment (Huh *et al*., 2002), and it is therefore likely that the prevention of this process contributed to the increased sensitivity of the GFP–AtAtg8f-HA plants to the mild salt stress compared with the control plants. The growth arrest of primary roots is generally associated with programmed cell death of the primary root meristem (Katsuhara and Kawasaki, 1996; Huh *et al*., 2002) and it is thus possible that expression of the GFP–AtAtg8f-HA construct negatively affects this programmed cell death by stimulating autophagy. This is supported by another independent study indicating that autophagy prevents the death of healthy uninfected cells during a plant defence response (Liu *et al*., 2005; Patel *et al*., 2006). Hence, the results imply that inactivation of the basal autophagy is required for proper inhibition of primary root growth in response to salt stress.

### *GFP–AtAtg8f-HA expression stimulates cell proliferation in ageing roots following exposure to osmotic stress*

Prolonged exposure to osmotic stress induced the widening of ageing roots and formation of globular structures along the primary roots of the GFP–AtAtg8f-HA-expressing plants, but not of the control plants. These phenotypes were largely due to extensive cell proliferation in the

vicinity of the xylem and phloem. Although the nature of these proliferated cells is as yet unclear, it is hypothesized that this phenomenon is also associated with a cross-reaction between GFP–AtAtg8f-HA expression and cytokinin signalling due to the following: (i) cytokinins are known to be associated with the proliferation of undifferentiated cells in plants (den Boer and Murray, 2000); (ii) cytokinins were documented to stimulate genes controlling cell cycle progression in roots (den Boer and Murray, 2000); and (iii) the globular structures observed on the roots of the GFP–AtAtg8f-HA-expressing plants resemble in their morphology the nodules formed on legume roots in response to rhizobia infection, a process that is also controlled by cytokinins (Murray *et al*., 2007; Tirichine *et al*., 2007).

## Supplementary data

Supplementary figures for this manuscript are available at *JXB* online.

Supplementary Fig. S1 illustrates that application of the cytokinin molecule zeatin (100 ng $ml^{-1}$) to the growth medium causes enhanced anthocyanin accumulation in shoots of the GFP–AtAtg8f-HA-expressing plants, compared with the control plants, as determined by increased red colour in the shoots and in extracts from shoots.

Supplementary Fig. S2 illustrates that the GFP–AtAtg8f-HA and the control plants show comparable responses to relatively severe salt (150 mM NaCl) and osmotic (150 mM mannitol) stresses.

## Acknowledgements

We thank Professor Zvulun Elazar for his helpful comments and Professor Ron Aloni for his invaluable help with the microscopic analysis of roots. The electron microscopy studies were conducted at the Irving and Cherna Moskowitz Center for Nano and Bio-Nano Imaging at the Weizmann Institute of Science. This research was supported by The United States–Israel Binational Science Foundation (BSF) Grant no. 1999-355, and by the European Union Research Training Network Contract no. HPRN-CT-2002-00262. GG is an incumbent of the Bronfman Chair in Plant Sciences.

## References

**Aloni R, Aloni E, Langhans M, Ullrich CI.** 2006. Role of cytokinin and auxin in shaping root architecture: regulating vascular differentiation, lateral root initiation, root apical dominance and root gravitropism. *Annals of Botany* **97,** 883–893.

**Bassham DC.** 2007. Plant autophagy—more than a starvation response. *Current Opinion in Plant Biology* **10,** 587–593.

**Bassham DC, Laporte M, Marty F, Moriyasu Y, Ohsumi Y, Olsen LJ, Yoshimoto K.** 2006. Autophagy in development and stress responses of plants. *Autophagy* **2,** 2–11.

**Brady SM, Orlando DA, Lee JY, Wang JY, Koch J, Dinneny JR, Mace D, Ohler U, Benfey PN.** 2007. A high-resolution root spatiotemporal map reveals dominant expression patterns. *Science* **318,** 801–806.

**Cao WH, Liu J, He XJ, Mu RL, Zhou HL, Chen SY, Zhang JS.** 2007. Modulation of ethylene responses affects plant salt-stress responses. *Plant Physiology* **143,** 707–719.

**Chen CG, Li JG, Chen Y, Huang P, Wang YL, Liu-Chen LY.** 2006. GEC1 interacts with the kappa opioid receptor and enhances expression of the receptor. *Journal of Biological Chemistry* **281,** 7983–7993.

**Contento AL, Xiong Y, Bassham DC.** 2005. Visualization of autophagy in Arabidopsis using the fluorescent dye monodansylcadaverine and a GFP–AtATG8e fusion protein. *The Plant Journal* **42,** 598–608.

**Deikman J, Hammer PE.** 1995. Induction of anthocyanin accumulation by cytokinins in Arabidopsis thaliana. *Plant Physiology* **108,** 47–57.

**den Boer BGW, Murray JAH.** 2000. Triggering the cell cycle in plants. *Trends in Cell Biology* **10,** 245–250.

**Doelling JH, Walker JM, Friedman EM, Thompson AR, Vierstra RD.** 2002. The APG8/12-activating enzyme APG7 is required for proper nutrient recycling and senescence in Arabidopsis thaliana. *Journal of Biological Chemistry* **277,** 33105–33114.

**Downes B, Vierstra RD.** 2005. Post-translational regulation in plants employing a diverse set of polypeptide tags. *Biochemistry Society Transactions* **33,** 393–399.

**Drose S, Bindseil KU, Bowman EJ, Siebers A, Zeeck A, Altendorf K.** 1993. Inhibitory effect of modified bafilomycins and concanamycins on P- and V-type adenosinetriphosphatases. *Biochemistry* **32,** 3902–3906.

**Elazar Z, Scherz-Shouval R, Shorer H.** 2003. Involvement of LMA1 and GATE-16 family members in intracellular membrane dynamics. *Biochimica et Biophysica Acta* **1641,** 145–156.

**Forde BG.** 2002. Local and long-range signaling pathways regulating plant responses to nitrate. *Annual Review of Plant Biology* **53,** 203–224.

**Franco-Zorrilla JM, Martin AC, Leyva A, Par-Ares JP.** 2005. Interaction between phosphate-starvation, sugar, and cytokinin signaling in arabidopsis and the roles of cytokinin receptors CRE1/AHK4 and AHK3. *Plant Physiology* **138,** 847–857.

**Fujita M, Fujita Y, Noutoshi Y, Takahashi F, Narusaka Y, Yamaguchi-Shinozaki K, Shinozaki K.** 2006. Crosstalk between abiotic and biotic stress responses: a current view from the points of convergence in the stress signaling networks. *Current Opinion in Plant Biology* **9,** 436–442.

**Gan SS, Amasino RM.** 1995. Inhibition of leaf senescence by autoregulated production of cytokinin. *Science* **270,** 1986–1988.

**Geldner N, Anders N, Wolters H, Keicher J, Kornberger W, Muller P, Delbarre A, Ueda T, Nakano A, Jurgens G.** 2003. The Arabidopsis GNOM ARF-GEF mediates endosomal recycling, auxin transport, and auxin-dependent plant growth. *Cell* **112,** 219–230.

**Geldner N, Friml J, Stierhof YD, Jurgens G, Palme K.** 2001. Auxin transport inhibitors block PIN1 cycling and vesicle trafficking. *Nature* **413,** 425–428.

**Glover BJ, Torney K, Wilkins CG, Hanke DE.** 2008. CYTOKININ INSENSITIVE-1 regulates levels of different forms of cytokinin in Arabidopsis and mediates response to nutrient stress. *Journal of Plant Physiology* **165,** 251–261.

**Grebe M, Friml J, Swarup R, Ljung K, Sandberg G, Terlou M, Palme K, Bennett MJ, Scheres B.** 2002. Cell polarity signaling in Arabidopsis involves a BFA-sensitive auxin influx pathway. *Current Biology* **12,** 329–334.

**Hanaoka H, Noda T, Shirano Y, Kato T, Hayashi H, Shibata D, Tabata S, Ohsumi Y.** 2002. Leaf senescence and starvation-

induced chlorosis are accelerated by the disruption of an Arabidopsis autophagy gene. *Plant Physiology* **129,** 1181–1193.

**Hirose N, Takei K, Kuroha T, Kamada-Nobusada T, Hayashi H, Sakakibara H.** 2008. Regulation of cytokinin biosynthesis, compartmentalization and translocation. *Journal of Experimental Botany* **59,** 75–83.

**Holton TA, Cornish EC.** 1995. Genetics and biochemistry of anthocyanin biosynthesis. *The Plant Cell* **7,** 1071–1083.

**Huang WP, Klionsky DJ.** 2002. Autophagy in yeast: a review of the molecular machinery. *Cell Structure and Function* **27,** 409–420.

**Huh GH, Damsz B, Matsumoto TK, Reddy MP, Rus AM, Ibeas JI, Narasimhan ML, Bressan RA, Hasegawa PM.** 2002. Salt causes ion disequilibrium-induced programmed cell death in yeast and plants. *The Plant Journal* **29,** 649–659.

**Inoue Y, Suzuki T, Hattori M, Yoshimoto K, Ohsumi Y, Moriyasu Y.** 2006. AtATG genes, homologs of yeast autophagy genes, are involved in constitutive autophagy in Arabidopsis root tip cells. *Plant and Cell Physiology* **47,** 1641–1652.

**Kanematsu T, Mizokami A, Watanabe K, Hirata M.** 2007. Regulation of GABA(A)-receptor surface expression with special reference to the involvement of GABARAP (GABA(A) receptor-associated protein) and PRIP (phospholipase C-related, but catalytically inactive protein). *Journal of Pharmacological Science* **104,** 285–292.

**Katsuhara M, Kawasaki T.** 1996. Salt stress induced nuclear and DNA degradation in meristematic cells of barley roots. *Plant and Cell Physiology* **37,** 169–173.

**Ketelaar T, Voss C, Dimmock SA, Thumm M, Hussey PJ.** 2004. Arabidopsis homologues of the autophagy protein Atg8 are a novel family of microtubule binding proteins. *FEBS Letters* **567,** 302–306.

**Laxmi A, Paul LK, Raychaudhuri A, Peters JL, Khurana JP.** 2006. Arabidopsis cytokinin-resistant mutant, cnr1, displays altered auxin responses and sugar sensitivity. *Plant Molecular Biology* **62,** 409–425.

**Legesse-Miller A, Sagiv Y, Porat A, Elazar Z.** 1998. Isolation and characterization of a novel low molecular weight protein involved in intra-Golgi traffic. *Journal of Biological Chemistry* **273,** 3105–3109.

**Liu Y, Schiff M, Czymmek K, Talloczy Z, Levine B, Dinesh-Kumar SP.** 2005. Autophagy regulates programmed cell death during the plant innate immune response. *Cell* **121,** 567–577.

**Mann SS, Hammarback JA.** 1994. Molecular characterization of light chain-3—a microtubule-binding subunit of Map1a and Map1b. *Journal of Biological Chemistry* **269,** 11492–11497.

**Mansuy V, Boireau W, Fraichard A, Schlick JL, Jouvenot M, Delage-Mourroux R.** 2004. GEC1, a protein related to GABARAP, interacts with tubulin and GABA(A) receptor. *Biochemical and Biophysical Research Communications* **325,** 639–648.

**Merchan F, de Lorenzo L, Rizzo SG, Niebel A, Manyani H, Frugier F, Sousa C, Crespi M.** 2007. Identification of regulatory pathways involved in the reacquisition of root growth after salt stress in Medicago truncatula. *The Plant Journal* **51,** 1–17.

**Miyawaki K, Matsumoto-Kitano M, Kakimoto T.** 2004. Expression of cytokinin biosynthetic isopentenyltransferase genes in Arabidopsis: tissue specificity and regulation by auxin, cytokinin, and nitrate. *The Plant Journal* **37,** 128–138.

**Mizushima N, Ohsumi Y, Yoshimori T.** 2002. Autophagosome formation in mammalian cells. *Cell Structure and Function* **27,** 421–429.

**Moore B, Zhou L, Rolland F, Hall Q, Cheng WH, Liu YX, Hwang I, Jones T, Sheen J.** 2003. Role of the Arabidopsis glucose sensor HXK1 in nutrient, light, and hormonal signaling. *Science* **300,** 332–336.

**Muller JMM, Shorter J, Newman R, Deinhardt K, Sagiv Y, Elazar Z, Warren G, Shima DT.** 2002. Sequential SNARE disassembly and GATE-16–GOS-28 complex assembly mediated by distinct NSF activities drives Golgi membrane fusion. *Journal of Cell Biology* **157,** 1161–1173.

**Murray JD, Karas BJ, Sato S, Tabata S, Amyot L, Szczyglowski K.** 2007. A cytokinin perception mutant colonized by Rhizobium in the absence of nodule organogenesis. *Science* **315,** 101–104.

**Nitsch JP.** 1970. Experimental androgenesis in Nicotiana. *Phytomorphology* **19,** 389–404.

**Ohshiro K, Rayala SK, Kondo S, Gaur A, Vadlamudi RK, El-Naggar AK, Kumar R.** 2007. Identifying the estrogen receptor coactivator PELP1 in autophagosomes. *Cancer Research* **67,** 8164–8171.

**Pankiv S, Clausen TH, Lamark T, Brech A, Bruun JA, Outzen H, Overvatn A, Bjorkoy G, Johansen T.** 2007. p62/SQSTM1 binds directly to Atg8/LC3 to facilitate degradation of ubiquitinated protein aggregates by autophagy. *Journal of Biological Chemistry* **282,** 24131–24145.

**Patel S, Caplan J, Dinesh-Kumar SP.** 2006. Autophagy in the control of programmed cell death. *Current Opinion in Plant Biology* **9,** 391–396.

**Phillips AR, Suttangkakul A, Vierstra RD.** 2008. The ATG12 conjugating enzyme ATG10 is essential for autophagic vesicle formation in Arabidopsis thaliana. *Genetics* **178,** 1339–1353.

**Sakakibara H.** 2006. Cytokinins: activity, biosynthesis, and translocation. *Annual Review of Plant Biology* **57,** 431–449.

**Sakakibara H, Takei K, Hirose N.** 2006. Interactions between nitrogen and cytokinin in the regulation of metabolism and development. *Trends in Plant Science* **11,** 440–448.

**Samuelson ME, Larsson CM.** 1993. Nitrate regulation of zeatin riboside levels in barley roots – effects of inhibitors of N-assimilation and comparison with ammonium. *Plant Science* **93,** 77–84.

**Sanchez DH, Siahpoosh MR, Roessner U, Udvardi M, Kopka J.** 2008. Plant metabolomics reveals conserved and divergent metabolic responses to salinity. *Physiologia Plantarum* **132,** 209–219.

**Scherz-Shouval R, Elazar Z.** 2007. ROS, mitochondria and the regulation of autophagy. *Trends in Cell Biology* **17,** 422–427.

**Shintani T, Klionsky DJ.** 2004. Autophagy in health and disease: a double-edged sword. *Science* **306,** 990–995.

**Shulaev V, Cortes D, Miller G, Mittler R.** 2008. Metabolomics for plant stress response. *Physiologia Plantarum* **132,** 199–208.

**Singh ST, Letham DS, Zhang XD, Palni LMS.** 1992. Cytokinin biochemistry in relation to leaf senescence. 6. Effect of nitrogenous nutrients on cytokinin levels and senescence of tobacco-leaves. *Physiologia Plantarum* **84,** 262–268.

**Slavikova S, Shy G, Yao YL, Giozman R, Levanony H, Pietrokovski S, Elazar Z, Galili G.** 2005. The autophagy-associated Atg8 gene family operates both under favourable growth conditions and under starvation stresses in Arabidopsis plants. *Journal of Experimental Botany* **56,** 2839–2849.

**Stromhaug PE, Klionsky DJ.** 2001. Approaching the molecular mechanism of autophagy. *Traffic* **2,** 524–531.

**Su W, Ma HJ, Liu C, Wu JX, Yang JS.** 2006. Identification and characterization of two rice autophagy associated genes, OsAtg8 and OsAtg4. *Molecular Biology Reports* **33,** 273–278.

**Takei K, Sakakibara H, Taniguchi M, Sugiyama T.** 2001. Nitrogen-dependent accumulation of cytokinins in root and the translocation to leaf: implication of cytokinin species that induces gene expression of maize response regulator. *Plant and Cell Physiology* **42,** 85–93.

**Takei K, Ueda N, Aoki K, Kuromori T, Hirayama T, Shinozaki K, Yamaya T, Sakakibara H.** 2004. AtIPT3 is a key determinant of nitrate-dependent cytokinin biosynthesis in Arabidopsis. *Plant and Cell Physiology* **45,** 1053–1062.

**Thompson AR, Vierstra RD.** 2005. Autophagic recycling: lessons from yeast help define the process in plants. *Current Opinion in Plant Biology* **8,** 165–173.

**Tirichine L, Sandal N, Madsen LH, Radutoiu S, Albrektsen AS, Sato S, Asamizu E, Tabata S, Stougaard J.** 2007. A gain-of-function mutation in a cytokinin receptor triggers spontaneous root nodule organogenesis. *Science* **315,** 104–107.

**Toyooka K, Moriyasu Y, Goto Y, Takeuchi M, Fukuda H, Matsuoka K.** 2006. Protein aggregates are transported to vacuoles by a macroautophagic mechanism in nutrient-starved plant cells. *Autophagy* **2,** 96–106.

**Wagner BM, Beck E.** 1993. Cytokinins in the perennial herb Urtica dioica L as influenced by its nitrogen status. *Planta* **190,** 511–518.

**Wang H, Bedford FK, Brandon NJ, Moss SJ, Olsen RW.** 1999. GABA(A)-receptor-associated protein links GABA(A) receptors and the cytoskeleton. *Nature* **397,** 69–72.

**Wang CW, Klionsky DJ.** 2003. The molecular mechanism of autophagy. *Molecular Medicine* **9,** 65–76.

**Wang H, Olsen RW.** 2000. Binding of the GABA(A) receptor-associated protein (GABARAP) to microtubules and microfilaments suggests involvement of the cytoskeleton in GABARAP-GABA(A) receptor interaction. *Journal of Neurochemistry* **75,** 644–655.

**Xie ZP, Klionsky DJ.** 2007. Autophagosome formation: core machinery and adaptations. *Nature Cell Biology* **9,** 1102–1109.

**Xiong Y, Contento AL, Nguyen PQ, Bassham DC.** 2007. Degradation of oxidized proteins by autophagy during oxidative stress in Arabidopsis. *Plant Physiology* **143,** 291–299.

**Yoshimoto K, Hanaoka H, Sato S, Kato T, Tabata S, Noda T, Ohsumi Y.** 2004. Processing of ATG8s, ubiquitin-like proteins, and their deconjugation by ATG4s are essential for plant autophagy. *The Plant Cell* **16,** 2967–2983.